



Published in final edited form as:

Virology. 2015 February ; 476: 115–123. doi:10.1016/j.virol.2014.11.028.

Genetics of Critical Contacts and Clashes in the DNA Packaging Specificities of Bacteriophages λ and 21

Jean Sippy^{*,a}, Priyal Patel^b, Nicole Vahanian^a, Rachel Sippy^c, and Michael Feiss^a

Abstract

The *cos* sites in λ and 21 chromosomes contain binding sites that recruit terminase to initiate DNA packaging. The small subunits of terminase, gpNu1 (λ) and gp1 (21), have winged helix-turn-helix DNA binding domains, where the recognition helices differ in four of nine residues. To initiate packaging, the small subunit binds three R sequences in the *cosB* subsite. λ and 21 cannot package each other's DNA, due to recognition helix and R sequence differences. In λ and 21 *cosBs*, two bp, tri1 and tri2, are conserved in the R sequences yet differ between the phages; they are proposed to play a role in phage-specific packaging by λ and 21. Genetic experiments done with mixed and matched terminase and *cosB* alleles show packaging specificity depends on favorable contacts and clashes. These interactions indicate that the recognition helices orient with residues 20 and 24 proximal to tri2 and tri1, respectively.

Keywords

Terminase; Virus assembly; DNA recognition; Viral packaging; TerS

Introduction¹

In a critical early stage of virus genome packaging, viral chromosomes are selected from a nucleic acid pool that may include the host's nucleic acids and, at times, those of other viruses. For the large dsDNA viruses, including the herpesviruses and the tailed bacteriophages, the viral terminase enzyme specifically recognizes viral DNA, selecting it for translocation into the preformed empty shell, the prohead (Casjens, 2011, Catalano et al., 1995, Feiss, 2012). DNA replication by many of these viruses produces end-to-end concatemers of viral DNA that are cut during packaging, generating virion chromosomes.

*Corresponding author. Phone: (319) 335-8866. Fax: (319) 335-9006. jean-sippy@uiowa.edu.

^aPresent addresses: Department of Microbiology, 51 Newton Road, Roy J. and Lucille A. Carver College of Medicine, University of Iowa, Iowa City IA 52242, vahanian.nicole@gmail.com, michael-feiss@uiowa.edu

^bPresent addresses: University Hospitals and Clinics (UIHC) 200 Hawkins Dr. Department of Pathology 6240 RCP, Iowa City IA 52242, priyal-patel@uiowa.edu

^cPresent addresses: Department of Population Health Sciences, University of Wisconsin-Madison, 610 North Walnut Street, Madison, WI 53726, sippy@wisc.edu

¹Amino acids are designated by one letter. Coordinates of the λ genome are according to Daniels et al. (Daniels et al., 1983). Bp = base pair(s). Kn = kanamycin. Ap = ampicillin. TerS and TerL indicate the small and large terminase subunits, respectively. wHTH = winged helix-turn-helix DNA binding motif. *NuI^{hy1}* has a chimeric *NuI* gene in which the recognition helix is that of 21 and the remainder of the coding sequence is from λ . For *NuI^{hy2}*, the N-terminal tail (4 residues), support helix, turn and recognition helix are from 21, and the remainder is from λ . For clarity, the origins of DNA binding domain segments will be indicated, where N = N-terminal tail, HTH = support helix, turn, and recognition helix, i.e., *NuI^{hy1}* is N ^{λ} H ^{λ} T ^{λ} H²¹, and *NuI^{hy2}* is N²¹H²¹T²¹H²¹. Mutations causing amino acid changes will be designated in superscripts, such as *NuI^{E24V}*.

Terminase sponsors both the endonucleolytic processing and translocation of viral DNA into the prohead. Terminases are generally hetero-oligomers of a small subunit involved in specific binding of viral DNA, and a large subunit. The large subunit is multifunctional, consisting of an N-terminal ATPase domain, a C-terminal endonuclease domain that cuts the concatemer into mature virion chromosomes, and the ATP-powered motor involving both domains (Casjens, 2011, Feiss and Catalano, 2005, Rao and Feiss, 2008).

dsDNA phages process concatemeric DNA using several strategies. In the headful mechanism, TerS binds the *pac* site, positioning the TerL's endonuclease to make a nearby dsDNA break, followed in turn by DNA translocation sponsored by TerL's ATP-powered translocase activity. The downstream DNA cleavage is made when the phage head is filled with slightly more than 100% of the unique genome sequence, producing a virion DNA with a terminally redundant sequence. For phages with specific DNA ends, like the cohesive ends of λ -like phage DNAs, TerS binds to a *cos* site along the concatemer, specifically the *cosB* subsite, positioning TerL for efficient and accurate introduction of staggered nicks into the adjacent *cosN* subsite, producing cohesive ends. Translocation proceeds to the next *cos*, at which point the downstream *cos* is nicked, completing packaging of the phage DNA molecule. For some phages, like λ and P22, TerS and TerL assemble into a holoterminase, whereas for other phages, like T3 and T4, the subunits act independently, associating only upon assembly of the DNA cleavage complex (Feiss and Catalano, 2005). TerS subunits form gear-shaped structures of radially disposed subunits. For the TerS oligomers with known structures, there are three domains, the first being an N-terminal domain containing a helix-turn-helix DNA binding motif. The central "core" domain is a cylinder of bundled α helices, followed by the cap, a small C-terminal β -barrel domain formed of parallel β strands (Buttner et al., 2012, Roy et al., 2012)(Buttner et al., 2012, Zhao et al., 2012). TerS recognizes *pac* or *cos* on viral DNA, and modulates TerL ATPase. A TerS controversy is whether virus DNA wraps around the DNA binding domains that are arrayed on the outside of the core, or whether the DNA is threaded thru the central channel. The width of the channel varies from phage to phage, and can be as narrow as 14.5Å (phage SF6), which is too narrow to accommodate a dsDNA molecule. A second controversy concerns the location of DNA binding motifs. Specific DNA binding has been inferred from powerful genetic experiments dissecting DNA packaging specificity, especially in λ -like and P22-like phages (Frackman et al., 1985)(Leavitt et al., 2013). *In vitro*, specific DNA binding by TerS has not been demonstrated. Rather, low affinity, non-specific DNA binding activity is generally found, including for TerS of P22. Complicating the genetics is the finding that removal of the C-terminal cap abolishes DNA binding, while not affecting oligomerization (Roy et al., 2012). The extensive genetic analysis shows that the C-termini of TerS oligomers function in contacts with TerL, but do not support a role for the cap in specific DNA binding.

For λ , gpNu1 and gpA form a stable heterooligomer, as follows. Following co-expression, a heterotrimer with the composition (gpNu1)₂:gpA can be recovered and shown to assemble into tetramers of heterotrimers [(gpNu1)₂:gpA]₄, a species that, it is argued, does not require further assembly or rearrangement for cutting *cosN* or sponsoring translocation (Maluf et al., 2005, Maluf et al., 2006). By analogy with the other TerS oligomers, it seems likely that assembly of the tetrameric form of terminase includes assembly of a gear-shaped gpNu1 octamer.

λ 's gpNu1 identifies viral DNA through interactions with the phage-specific *cosB* site. *cosB* is located downstream from *cosN*, the subsite where nicks, staggered by 12 bp, are introduced by the large terminase subunit, gpA, to generate virion genomes from concatemeric DNA. *cosB* ^{λ} has three R elements (R3, R2, and R1), with the 16 bp consensus sequence 5'-tGtCGTTTCCtTTCTt-3', where bp conserved in all three R sequences are capitalized (Figure 1). According to the current model, at the initiation of packaging, R3 and R2 are bound by a dimer of terminase's small subunit, gpNu1. The gpNu1 DNA binding domain is a wHTH motif (de Beer et al., 2002); sequences for a wHTH are also found in the small subunit of 21's terminase, gp1, along with those of many λ -like phages.

For phage 21, a relative of λ , the R sequences are very similar to λ 's (Figure 1), yet the two phages are able to discriminate quite efficiently against each other's DNA. Both λ - and 21-specific terminases exhibit 10³-to-10⁴-fold discrimination between self and non-self *cosB*-containing DNAs (Feiss et al., 1981).

Two bp of the λ and 21 R sequences differ between the two phages, yet are conserved in all three R sequences of each phage (Figure 1, Becker and Murialdo, 1990); these are underlined in the following consensus sequences: λ - 5'-tGtCGTTTCCtTTCTt-3' and 21: 5'-tTCaTGTCGNaCTT-3'. Becker and Murialdo proposed that these bp were likely important for recognition by the small terminase subunit, and also were likely involved in phage specific interactions that might account for discrimination against hetero-specific DNAs. Herein, we designate the upstream 5', conserved bp as the tri1 bp and the downstream, 3' conserved bp as tri2. Whether the bp at these positions are of λ or 21 origin will be indicated by superscripts, i.e., *tri1* ^{λ} or *tri2*²¹. In the present work, we investigated the roles of tri1 and tri2 in packaging specificity.

Results and Discussion

Strategy

In order to test the idea that *cosB* specificity involves tri1 and/or tri2, we changed the *cosB* ^{λ} bp at the tri1 and tri2 positions to those of 21, creating *cosB* ^{λ} *hexa*²¹. Additionally, we looked at the effects of swapping λ -specific bp for the 21-specific bp at the tri1 and tri2 positions in each R element, creating *cosB* ^{λ} *tri1*²¹ and *cosB* ^{λ} *tri2*²¹ mutants (Figure 1). These *cosB* changes were then mixed and matched with *NuI* alleles: *NuI*⁺, *NuI*^{hy1} (N ^{λ} H ^{λ} T ^{λ} H²¹) and *NuI*^{hy2} (N²¹H²¹T²¹H²¹), and the resulting phages were studied by determining burst sizes (Table 2). The *NuI*^{hy1} is identical to *NuI*⁺ except that the codons for the four amino acids by which λ 's recognition helix differs from that of 21 have been swapped out (Figure 2). Previous work shows that this terminase efficiently packages 21 DNA, but discriminates against λ DNA poorly, showing only about a 10-fold preference for 21 DNA. *NuI*^{hy2} terminase contains the N-terminus and the helix-turn-helix motif from 21, with the remainder of the protein identical to gpNu1. The wing motif of *NuI*^{hy2} is from gpNu1. Previous work has shown that wing function is not phage-specific (Feiss et al., 2010). *NuI*^{hy2} terminase packages 21 DNA efficiently, and discriminates against λ DNA with the same stringency as phage 21 holoterminase (Feiss et al., 1981).

For lethal combinations of *cosB* and *NuI* alleles, pseudorevertants were isolated and sequenced to determine the sorts of changes that permitted plaque-formation (Table 3). We also created four modified gpNu1s by swapping each of the four differing amino acids in the recognition helix with those of 21 gp1; their effects on phage viability were determined (Table 4). Finally, a cosmid packaging experiment tested a model that E20 of 21's recognition helix clashes with *tri2*^λ (Table 5). Interpretations are based on the known dependence of specificity on interactions between bp and amino acid R groups, and that these interactions can be energetically favorable contacts that enhance terminase binding or negative interactions stemming from steric or charge clashes that interfere with binding. It is further expected that some R sequence bp and amino acids of the recognition helix will simply not make critical contacts. While we assumed that the genetic effects of bp and amino acid changes would generate a data set that could be interpreted in terms of these interactions, we also recognized that amino acid changes may also have local effects on the positioning of neighboring residues, protein folding, multimer assembly, etc.

Changing the conserved, phage-specific *tri1* and *tri2* bp of *cosB*^λ swaps packaging specificity

Changing the *tri1* and *tri2* bp of *cosB*^λ into the corresponding bp of the 21 R sequence (*cosB*^λ *hexa*²¹) enabled efficient packaging by 21-specific *NuI*^{hy1} (N^λH^λT^λH²¹) and *NuI*^{hy2} (N²¹H²¹T²¹H²¹) terminases (Table 2, lines 2 and 3), indicating that one or both bp are critical for recognition. As found previously, the gpNu1^{hy1} terminase (N^λH^λT^λH²¹) did not discriminate strongly, packaging *cosB*^λ DNA with about 10% the efficiency of *cosB*²¹ DNA (Table 2, line 2). For gpNu1^{hy1} terminase, either the *tri1*²¹ or *tri2*²¹ changes to *cosB*^λ resulted in efficient packaging. For gpNu1^{hy2} terminase (N²¹H²¹T²¹H²¹), the *tri1*²¹ and *tri2*²¹ changes to *cosB*^λ improved packaging significantly, by factors of 250 and 800, resp., but both changes were required for 100% efficiency. We conclude that *tri1*²¹ and *tri2*²¹ are critical for *cosB*²¹ recognition by 21-specific terminase. These observations by themselves are consistent with both favorable-contact and/or clash-relief explanations for the 21-specific packaging enhancement produced by *tri1*²¹ and *tri2*²¹.

Discrimination by λ and 21-specific terminases

Wild type λ terminase packaged *cosB*²¹ DNA very poorly (0.03%) as observed previously (Table 2) (de Beer et al., 2002, Feiss et al., 1981). The yield of λ *NuI*⁺ *cosB*^λ *hexa*²¹, with the *tri*^λ-to-*tri*²¹ changes, was reduced about 10-fold compared with λ *NuI*⁺ *cosB*^λ. A similar yield reduction was observed for λ *NuI*⁺ *cosB*^λ *tri1*²¹ but not for λ *NuI*⁺ *cosB*^λ *tri2*²¹. Thus λ terminase is indifferent to the specificity at the *tri2* position, but requires *tri1*^λ for efficient packaging. These results indicate that λ terminase may have a clash with *tri1*²¹, and/or make a specific contact with *tri1*^λ.

With respect to discrimination, both the *NuI*⁺ and *NuI*^{hy2} terminases, which discriminate strongly against packaging chromosomes with the wild type heterospecific *cosB*, packaged chromosomes with the *cosB*^λ *hexa*²¹ changes much better than *cosB*²¹ and *cosB*^λ chromosomes, resp. The observation that *NuI*^{hy2} terminase packages *cosB*^λ *hexa*²¹ chromosomes with full efficiency indicates that the *tri1*^λ and *tri2*^λ bp of *cosB*^λ are major factors by which *NuI*^{hy2} terminase discriminates against heterospecific *cosB*^λ

chromosomes. That is, the unchanged, non-*tri* bp of the *cosB*^λ R sequences in *cosB*^λ *hexa*²¹ do not interfere with packaging of *cosB*^λ *hexa*²¹ chromosomes by the 21-specific terminases. On the other hand, λ's *NuI*⁺ terminase, which packages *cosB*^λ *hexa*²¹ chromosomes with intermediate efficiency, must recognize additional bp of the 21-specific R sequences in discriminating against 21-specific DNA. The observation that *tri*²¹ did not reduce the efficiency of packaging by *NuI*⁺ terminase indicates that if the *tri*^λ bp is contacted by gpNu1, both the CG bp of *tri*^λ and the GC bp of *tri*²¹ are contacted.

gpNu1's E24 clashes with *tri*²¹ and forms a favorable contact with *tri*^λ

λ *cosB*^λ *hexa*²¹ is unable to form plaques. We isolated 59 independent pseudorevertants and determined the sequences to find out what changes permitted plaque formation (Table 3). All 20 of the variants with *cosB* changes had reversion mutations of a *tri*²¹ bp back to the λ bp, either in R3 (G56T, 17 isolates) or R2 (C117A; 3 isolates). That all 20 variants had changes to a *tri*^λ bp indicates that these changes relieve a clash and also create a favorable contact. In the unlikely alternative explanation where these *tri*²¹-to-*tri*^λ changes simply relieve the clash, the other possible changes at *tri*, i.e., to CG and AT, would be expected to be observed.

The remaining changes in plaque-forming revertants of λ *cosB*^λ *hexa*²¹ were *NuI* mutations. Two non-conservative changes of residue 24 were *NuI*^{E24V} and *NuI*^{E24Q}. Both changes are to uncharged residues with very different side chains, suggesting that the E24's charged carboxyl is involved in the clash with *tri*²¹.

Additional variants with changes that compensate for the gpNu1 E24-*tri*²¹ clash

Several plaque forming variants of λ *cosB*^λ *hexa*²¹ had mutations changing recognition helix residues into basic residues; these were *NuI*^{N21K}, *NuI*^{E24K}, and *NuI*^{Q25K} (Table 3). These changes likely create favorable charge interactions with DNA backbone phosphates. Note that, barring altered recognition helix structure or orientation, for the *NuI*^{N21K} and *NuI*^{Q25K} changes, the E24-*tri*²¹ clash remains and must be compensated for. Finally, four of the remaining five variants contained known general suppressors of *cos* defects: *NuI*^{A14V} is also a suppressor of gpNu1 *NuI*^{K35A}, a mutant terminase with post-cleavage DNA binding defects (Hwang and Feiss, 1997) *NuI*^{L40F}, *NuI*^{L40I} and *NuI*^{Q97K} have been described as suppressors of lethal R sequence mutations (Cai, 1993, Cai et al., 1997). The *NuI*^{D104G} change, being in the vicinity of Q97, may also be a general suppressor, but it has not been studied further.

Two other reversion studies were carried out using stocks of λ *NuI*^{hy2} *tri*²¹ and λ *NuI*^{hy2} *tri*²¹ grown on a *mutD* host to increase the frequency of pseudorevertants. In our experience, mutations that compensate for lethal gpNu1 defects are located in the *NuI* gene, and each pseudorevertant contained a single *NuI* mutation, as follows. Pseudorevertants of λ *NuI*^{hy2} *tri*²¹ carried missense mutations: D₁₅V, a change in the turn; Q₂₃K (two isolates), and V₃₉L at the base of the wing. Q₂₃K was also found in a pseudorevertant of λ *NuI*^{hy1} *cosB*^λ (de Beer et al., 2002). Pseudorevertants of λ *NuI*^{hy2} *tri*²¹ included K₂E, which changes a charged residue in the 21-derived N-terminal tail of *NuI*^{hy2} to that of λ's N-terminal tail (MKNV→MENV).

Pseudorevertants of λ *NuI*⁺ *cosB* ^{λ} *hexa*²¹ contain suppressors of varying strengths

The burst sizes of λ *NuI*⁺ *cosB* ^{λ} *hexa*²¹ pseudorevertants were very variable. Variants with the general suppressors *NuI*^{L40F}, *NuI*^{L40I} and *NuI*^{Q97K} were the healthiest (Table 3). Observations of the ATPase activities and protease susceptibilities of the L40F terminase indicated that the conformation of gpNu1 is altered (Cai, 1993, Cai et al., 1997), a change that could compensate for the gpNu1 E24-*triI*²¹ clash. The next healthiest group of variants (burst sizes 44 to 59) contain alterations of E24, directly relieving the gpNu1 E24-*triI*²¹ clash. Pseudorevertants with burst sizes of ~30 include D104G and the G56T change in *cosB*'s R3. The least robust pseudorevertants, with the lowest burst sizes, were *NuI*⁺ *cosB* ^{λ} *hexa*²¹ → C₁₁₇A, *NuI*^{A14V}, and *NuI*^{N21K}. These pseudorevertants have burst sizes near that of the λ *NuI*⁺ *cosB* ^{λ} *hexa*²¹ parent phage from which they were isolated. The burst size of λ *NuI*⁺ *cosB* ^{λ} *hexa*²¹ is just below the threshold required for plaque formation, so very mild changes that permit formation of a tiny plaque are expected to have very minor increases in burst size, a difference too small to demonstrate with statistical significance. A number of studies indicate that gpNu1 binding to R3 is critical for DNA packaging (Cue and Feiss, 1992, Hang et al., 2001, Higgins and Becker, 1994), and so it is not surprising that the R3 change G56T is a stronger suppressor than the R3 change C117A.

A clash between 21's E20 and *cosB* ^{λ}

To ask about the interactions of individual residues of the recognition helix with R sequences, we studied the effects of individually changing each of the four phage-specific codons of the gpNu1 recognition helix to the corresponding 21-specific codons. Three changes, *NuI*^{I16P}, *NuI*^{N21R}, and *NuI*^{E24S}, either had no effect or reduced the yield modestly, but the *NuI*^{Q20E} change dramatically reduced the yield by a factor of nearly 10⁴ (Table 4). The *NuI*^{Q20E} change reduced packaging of *cosB* ^{λ} DNA to a level similar to that found for wild type 21 terminase and *cosB* ^{λ} DNA, a result indicating that E20 of 21's gp1 plays a major role in discrimination by 21 terminase. Data indicating the existence of an E20 versus *cosB* ^{λ} clash were reported previously, as follows (de Beer et al., 2002). de Beer et al. found compensating mutations affecting gpNu1^{hy1} of λ *cosB* ^{λ} *NuI*^{hy1}, including the changes E₂₀D and E₂₀G. These changes suggested there was a clash between 21's E20 and *cosB* ^{λ} , because shortening the side chain or eliminating the carboxyl group relieved the E20-*cosB* ^{λ} clash. In support of this proposal, we found λ *cosB* ^{λ} *NuI*^{E20A} as a viable revertant of λ *cosB* ^{λ} *NuI*^{Q20E} (Table 4), a third example indicating that replacement of the E20 side chain dramatically enhances virion assembly. These three changes of the 21-specific E20 residue to less bulky and/or uncharged residues are consistent with the presence of a clash between 21's E20 and *cosB* ^{λ} .

Evidence for clashes and favorable contacts between gpNu1's E24/gp1's E20 and *cosB* ^{λ} /*cosB*²¹

Our genetic data identified two clashes, E24 ^{λ} -*triI*²¹ and E20²¹-*cosB* ^{λ} , and a favorable E24 ^{λ} -*triI* ^{λ} contact. To determine which bp of *cosB* ^{λ} clashes with E20²¹, a cosmid packaging experiment was done using Ap^R *cos* ^{λ} cosmids with *cosB*⁺, *triI*²¹, *triI*²¹, and *hexa*²¹ alleles as packaging substrates, and helper phages λ *cos*⁺ *NuI*⁺ and λ *cos*⁺ *NuI*^{Q20E}. The data (Table 5) were normalized to the wild type control where λ *cos*⁺ *NuI*⁺

packaged the *cosB*^λ cosmid. As found for *NuI*⁺ phages with these *cosB* alleles, packaging of *tri1*²¹ or *hexa*²¹ cosmids was sharply reduced, but the presence of *tri2*²¹ did not greatly affect packaging.

For λ *NuI*^{Q20E}, the most efficiently packaged cosmid was *cosB*^λ *tri2*²¹, indicating that E20 clashes with *tri2*^λ. For the *cosB*^λ and *cosB*^λ *hexa*²¹ cosmids, packaging was reduced a further 5-to-10 fold, consistent with the presence of a clash in each case (Table 5), and for *cosB*^λ *tri1*²¹, the yield was reduced a further 15-to-30 fold, consistent with the presence of clashes at both *tri1* and *tri2*. We conclude that E20's clash with *cosB*^λ is with *tri2*^λ. Surprisingly, the yield of *cosB*^λ *tri2*²¹ cosmids packaged by λ *NuI*^{Q20E} was only 3.3%, a yield much less than expected if the proper E20²¹-*tri2*²¹ combination was present. We do not understand this low yield. Among possible explanations are that the presence of E20 in an otherwise λ HTH motif might (1) affect the strength of an E20²¹-*tri2*²¹ interaction, (2) alter the architecture of the recognition helix, in turn affecting the strength of other interactions between the recognition helix and *cosB* bp, or perhaps (3) cause less efficient protein folding. One expects that all of these possible effects are present regardless of the cosmid's *cosB* allele.

The cosmid packaging data was further analyzed by assigning our proposed clashes and favorable interactions to each combination. We acknowledge the presence of other, unknown favorable or unfavorable contacts, and limit our interest here to interactions with *tri1* and *tri2*. As an analogy to a favorable contact of E24^λ with *tri1*^λ, we speculated there is a favorable E20²¹-*tri2*²¹ contact, and include it in this analysis. When the data is examined in this manner, it turns out that the packageability of a cosmid is consistent with the proposed clashes and favorable interactions, as outlined in Table 5. For example, λ *NuI*^{Q20E} *cosB*^λ *tri1*²¹ and λ *NuI*^{Q20E} *cosB*^λ both have the E20²¹-*tri2*^λ clash, yet packaging of λ *NuI*^{Q20E} *cosB*^λ is ~10-fold more efficient. We attribute this result to the presence, in the Q20E²¹-*cosB*^λ combination, of a favorable E24^λ-*tri1*^λ contact and the absence of the E24^λ-*tri1*²¹ clash. That a favorable E20²¹-*tri2*²¹ interaction exists is strengthened when comparing λ *NuI*^{Q20E} *cosB*^λ *tri2*²¹ (3.3% wild type) with λ *NuI*^{Q20E} *cosB*^λ (0.33% wild type)—the added favorable interaction accounts for the 10-fold difference in packageability for λ *NuI*^{Q20E} *cosB*^λ *tri2*²¹.

Is there a phage-specific contact by amino acid 2 of the N-terminus?

An additional interesting observation is that *NuI*^{hy1} terminase, which encodes gpNu1 with only the 21 recognition helix, discriminates between λ and 21 DNA much less well than does *NuI*^{hy2} terminase, which contains the entire 21 helix-turn-helix motif and N-terminal tail (Table 2, compare lines 2 and 3). We previously ascribed the difference to effects of the support helix and turn on positioning of the recognition helix. It is clear that the loss of discrimination is due to more efficient packaging of *cosB*^λ DNA by the *NuI*^{hy1} terminase, which in turn has a greater extent of the λ -specific DNA binding motif, namely the N-terminus, the support helix and the turn, than the *NuI*^{hy2} terminase. Modeling of the gpNu1 DNA binding domain with the R sequence indicates that the gpNu1 N-terminal tail is likely located near the DNA (de Beer et al., 2002). We note the dramatic residue difference - residue 2 is E in the λ -derived N-terminus of *NuI*^{hy1} and K in the 21-derived N terminus of

NuI^{hy2} (Figure 2). That this residue 2 difference might account for the increased ability of *NuI^{hy1}* terminase to package λ DNA relative to *NuI^{hy2}* terminase is supported by the recovery of the K₂E change in a pseudorevertant of λ *NuI^{hy2}cosB ^{λ} tri2²¹*. Systematic work is required on this issue, but the data suggest that residue 2 may be involved in packaging specificity.

Concluding Remarks

Genome recognition

Terminase small subunits generally consist of an N-terminal DNA-binding segment containing a HTH DNA binding motif, a central oligomerization domain of bundled α -helices, and a C-terminal barrel domain formed of parallel β -strands. The C-terminus contains the functional domain for binding the large terminase subunit (Yang et al., 1999). Terminase small subunits oligomerize into vase-shaped structures of radially disposed monomers. Though basic terminase structure is conserved among tailed phages, the small and large subunits show different assembly strategies. For λ terminase, the subunits assemble into a (gpNu1)₂:gpA₁ heterotrimer that further assembles, with the assistance of *cos* DNA, into a higher-order tetramer of heterotrimers that presumably contains a gpNu1 octamer. (Maluf et al., 2005, Maluf et al., 2006). In contrast, for phage T3, the small subunit binds the DNA and the large subunit assembles on the portal protein of the prohead, followed by construction of the complete packaging motor by the two precursor complexes (Fujisawa and Morita, 1997).

Helix orientation and the wing contact

We identified clashes between (1) E20 of phage 21's recognition helix and *tri2 ^{λ}* , and (2) E24 of the λ recognition helix and *tri1²¹*, a favorable contact between λ 's E24 and *tri1 ^{λ}* , and suggest a favorable contact between E20²¹ and *tri2²¹*. These interactions have implications regarding recognition helix orientation in the major groove upon binding by λ 's gpNu1 and 21's gp1. That is, the recognition helices of gpNu1 and gp1 could be positioned in the major groove such that residue 24 at the C-terminus of the helix is *tri1*-proximal and residue 20 is *tri2*-proximal. Figure 3 demonstrates the recognition helix placement for gpNu1 (a) and gp1 (b) in relation to their phage-specific base pairs. Our proposed placement of the recognition helix also orients the wing proximal to the DNA, as follows. The wing of gpNu1's DNA binding domain extends roughly at a right angle from the carboxy-end of the recognition helix (de Beer et al., 2002). Docking the recognition helix in the major groove in the orientation suggested here positions the wing hovering near the DNA downstream, or 3', to *tri2*, near bp 62-64: 5' AGGCGTTTCCGTTCTT-3', where *tri1* and *tri2* are underlined and T62, C63 and T64 are shaded (Figure 3). Since the wing is functionally not phage-specific (Feiss et al., 2010) it is interesting that bp 63 and 64 are conserved in all 6 R sequences of *cosB ^{λ}* and *cosB²¹*. Consistent with a proposal that the wing's K35 may contact a backbone phosphate, a prior mutant study (Hwang and Feiss, 1999) showed that gpNu1 K35A terminase had reduced binding strength and specificity. Two α -helices downstream of the wing, α -C and α -D, lie on the opposite side of the recognition helix from the wing (de Beer et al., 2002). In our model this would point the carboxy, gpA/gp2-interacting end of

gpNu1/gp1 toward *cosN* (Figure 3). This orientation is consistent with the positioning of gpA for cleavage of *cosN*; however, structural information is needed to verify this model.

Interactions of E24^λ and E20²¹ with base pairs

The carboxylate groups of E24^λ and E20²¹ likely interact with hydrogen donor groups of bases in the major groove. Though speculative, we propose possible amino acid-base interactions for E24^λ and E20²¹, as follows. Hydrogen bond donors are found in amino group N6 of adenine in *tri1^λ*, and the amino group N4 of cytosine in *tri1²¹* (Figure 3c). The amino acid-base interaction of E24^λ to *tri1^λ* could be an electrostatic interaction between the glutamate carboxylate with N6 of adenine at tri1 bp 56 on the bottom strand. Because the N4 amino group of cytosine at *tri1²¹* is similarly positioned, stereo-chemically, as *tri1^λ*'s N6 amino group, it is difficult to understand why E24^λ clashes with the *tri1²¹* GC bp. To explain the clash of E24^λ with *tri1²¹*, we propose that the C5 methyl group of *tri1^λ* thymine might be in a van der Waals interaction with the β or γ carbons of the E24^λ side chain. Thus, the E24^λ/*tri1²¹* clash may be due to the absence of this van der Waals interaction, resulting in positioning E24^λ to clash with the nearby hydrogen acceptors in the *tri2²¹* guanine (Steitz, 1990).

For E20²¹, the interaction with *tri2²¹* could be with N4 of the bottom strand cytosine. An E20²¹/*tri2^λ* clash would be created by O6 of λ's guanine, a hydrogen acceptor at the same geometric position as the hydrogen donating N4 of cytosine at bp 59 of *tri2²¹*.

The role of clashes in phage-specific DNA-protein interactions

Phages exchange segments and undergo genetic drift, processes that generate diversity. Divergence enables the creation of new specificities for transcriptional regulation, replication, prophage insertion, DNA packaging, etc. Divergence of these specificities lets phages avoid assisting competitors. In the present case, λ and 21 avoid packaging each other's DNA by virtue of having different packaging specificities. Such specificity differences are common, and as in the case of λ and 21 packaging specificities, amino acid-bp clashes are critical components. A case in point are the divergent specificities of the closely related RNA polymerases of phages T3 and T7 (Raskin et al., 1993). Though the two polymerases have 82% amino acid sequence identity, transcription by each is phage-specific. Combinatorial dissection of the promoters and promoter binding motifs shows that a single amino acid residue plays a critical role in phage specificity. In the specificity model of Raskin *et al.*, N748 of the T7 enzyme makes bridging contacts via hydrogen bonds with -10A and -11G of the T7 promoter (Raskin et al., 1993). The N748 amide is proposed to donate hydrogens to N7 and O6 of -11G and to accept a hydrogen bond from N6 of -10A. In T3, the corresponding amino acid, D747, forms bridges between -11C and -10C of the T3 promoter, and is proposed to accept hydrogens from the N4 nitrogens of -11C and -10C. Whether clashes play a role in the promoter specificity was not pursued, but it is likely that T7's N748 amide group may clash with the -11 N4 hydrogen of the T3 promoter. Similarly, T3's D749 might have a charge clash with the N7 and O6 hydrogens of -11G of the T7 promoter.

A second example is integrase specificity of phages λ and HK022, as follows. Dorgai et al. (Dorgai et al., 1995) suggest a clashing mechanism for specificity. Although they have ~70% sequence identity, the integrases of λ and phage HK022 catalyze nearly identical reactions, using different sets of DNA sites. Amino acids key to phage specificity were identified and it was found that substitution of HK022 for λ residues at five positions conferred almost complete HK022 recombinational specificity on λ integrase. Two of the changes broadened specificity and one of them, residue E319 of λ integrase tolerated a variety of changes which allowed λ integrase to recombine HK022 sites. The authors suggest that due to removal of a clash created by a negative charge, the E319R change alters the catalytic rate of the integrase.

Materials and Methods

Media, PCR, DNA sequencing, and competent bacterial strains

Luria broth (LB), Luria agar (LA), tryptone broth (TB), tryptone agar (TA), and tryptone soft agar (TBSA) were prepared as described (Arber, W., Enquist, L., Hohn, B., Murray, N. E., & Murray, K., 1983). TB, TA, and TBSA were supplemented with 0.01M MgSO₄. When required, kanamycin (Kn) and ampicillin (Ap) were used at final concentrations of 50 μ g/ml and 100 μ g/ml, respectively. PCR reactions were done using *Taq*Bead Hot Start Polymerase kit (Promega Inc.) and sequencing was done by The University of Iowa Institute of Human Genetics Genomic Division. PCR and sequencing primers were purchased from Integrated DNA Technologies (Coralville, IA). Competent cells for recombinant DNA manipulations were XL-10 (Stratagene) and DH5 α Library Efficiency (Invitrogen).

Phage, plasmids, and bacterial strains

The phage, plasmids, and bacterial strains mentioned in the text are listed in Table 1.

Constructing test phages with various *cosB* and *Nu1* alleles

Plasmid pJB0 is pBR322 (Bolivar et al., 1977) carrying the λ DNA segment that extends from the *Hind*III site at λ bp 44141, across *cos* and the terminase genes, to the *Bam*HI site at 5505. The pJB0 λ DNA segment contains introduced restriction sites for *Xba*I at 48442 and *Xma*I at 171, along with a natural *Mlu*I site at bp 458. The introduced sites flank *cos*, do not affect λ growth, and are useful for replacing *cos*, and the *Xma*I-to-*Mlu*I *Nu1* segment (Cue and Feiss, 1993, de Beer et al., 2002). pJB0 is *cos* λ^+ and *Nu1*⁺. Derivatives of pJB0 carrying these *cosB* λ alleles: *cosB* λ *hexa*²¹, *cosB* λ *tri1*²¹, and *cosB* λ *tri2*²¹ were constructed by replacing the *cosB* λ^+ segment using *Xba*I and *Xma*I. Similar derivatives carrying *Nu1*^{hy1} and *Nu1*^{hy2} alleles were constructed by replacing the *Nu1*⁺ segment using *Xma*I and *Mlu*I. In all a total of 12 such pJB0-based plasmids with all the possible combinations of *cosB* and *Nu1* alleles were used for crossing the *cosB* and *Nu1* alleles into phage. The *Nu1* alleles were described previously (de Beer et al., 2002) and the *Xba*I-to-*Xma*I segments with *cosB* λ *hexa*²¹, *cosB* λ *tri1*²¹, and *cosB* λ *tri2*²¹ alleles were from Blue Heron Biotechnology (Bothell, WA). Phage *versus* plasmid crosses were done to obtain recombinant λ -P1 *cosB* λ^i , *Nu1j* chimeric test phages, as follows. Chemically competent MF1427 (λ *cos2*) cells were prepared using the standard protocol (Maniatis, t., Fritsch, E. F., & Sambrook, J., 1982). The *cos2* mutation is a 22-bp deletion that removes *cosN* and consequently the prophage DNA

cannot be packaged (Cue and Feiss, 1992, Kobayashi et al., 1982). The lysogens were transformed with each of the pJB0-based plasmids (Table 1). Transformants were selected on LA + Ap plates at 31°C and grown at 31°C to 5×10^7 cells/ml. Next, the prophage was induced by shifting the culture to 42°C for 15 minutes, and the culture further incubated at 37°C for 70 min, at which time phage lysis had occurred. After treatment with CHCl_3 , the lysate was centrifuged to remove cell debris. Only recombinants which have picked up cosN^+ are packaged. To obtain recombinants, the Kn^R -transducing phages were selected as follows. A 100 μl aliquot of lysate was mixed with 0.2 ml of an overnight culture of MF1427. The mixture was incubated at room temp for 15 min, then diluted to 1 ml with LB. After an hour at 31°C, aliquots were spread on LA + Kn plates and incubated overnight at 31°C. Two isolates from each cross were selected for study after being screened for the presence of the desired *cosB* and *NuI* alleles by sequence analysis of PCR-generated DNA.

Determination of burst sizes of test phages

MF1427 lysogens of the λ phages of interest were grown at 31°C to $2\text{-}5 \times 10^7$ cells/ml. Aliquots of the cultures were diluted, and plated on TA plates at 30°C for a cell count. Prophage induction was at 42°C for 15 minutes. Cultures were then grown at 37°C for 70 minutes, treated with CHCl_3 , and clarified. Lysates were diluted and plated with MF1427 at 37°C for burst size assays, where burst sizes are defined as phages/induced cell. When phages were unable to make a plaque, the titer of Kn^R -transducing particles/ml was determined and adjusted using the efficiency of plating of wild type phage. To assay Kn^R -transducing phages, lysate dilutions were mixed with 200 μl of MF2979 cells and phages were allowed to adsorb at room temperature for 15 minutes. LB was added to 1.0 ml, and the cultures were incubated for 1 hour at 37°C. Aliquots of 200 μl were spread on LA + Kn plates and incubated at 37°C overnight.

Mutant phages with single amino acid replacements

Phages with single amino acid replacements were constructed using the same λ *cos2* × plasmid cross strategy used for test phage construction. Mutagenesis to create single amino acid replacement mutations was done using the QuikChange II Mutagenesis Kit (Stratagene), with pJB0 as template.

Cosmids for the cosmid packaging experiment (Table 5)

Cosmids were constructed using pJB4, an analogue of pJB0 deleted for the late promoter by removing the 832 bp-long, late promoter-containing *EcoRI* fragment that extends from pBR322 bp 43591 to λ bp 44942. Deleting the λ late promoter prevents expression of the cosmid terminase genes.

Cosmid packaging assay

Cosmids pJB0 *cosB* $^\lambda$, pJB0 *cosB* $^\lambda$ *hexa*²¹, pJB0 *cosB* $^\lambda$ *tri1*²¹, and pJB0 *cosB* $^\lambda$ *tri2*²¹ were transformed into competent MF1427 (λ *NuI*⁺ or λ *NuI* *Q*^{20E}) cells. The Ap^R Kn^R cells were grown and induced, and the lysate collected, as described in the Constructing Test Phages section. 100 μl of lysate and 100 μl of MF2979 cells were allowed to incubate for 15 minutes at room temperature, then LB was added to a final volume of 1.0 ml. After 1 hour of

incubation at 31°C, dilutions were spread on LA + Ap plates, and incubated overnight at 37°C.

Isolating revertants

Plaque-forming pseudorevertants were isolated on MF1427 cells by plating 100µl of lysate at 37°C. To make lysogens with the pseudorevertants, plaque suspensions were mixed with MF1427 cells which were then allowed to incubate at 31°C for one hour, and plated on LB + Kn plates at 31°C. The Kn^R colonies were used as template in PCR reactions, the products of which were used for sequencing analysis to determine the second-site mutation. The pseudorevertants of λ *cosB*^λ *tri1*²¹ *NuI*^{hy2} and λ *cosB*^λ *tri2*²¹ *NuI*^{hy2} were found in lysates made on the *mutD* strain MF2449.

Acknowledgement

We thank Grace Sippy for preparing Figures 3 (a) and (b), and Xuan-Loc V. Nguyen and Jamie Potter for strain constructions. This long-term project was supported by funding from NSF awards MCB-0717620 and MCB-1158495, NIH awards 5R01GM088186 and 5R01GM051611, and The University of Iowa Department of Microbiology.

Bibliography

- Arber, W.; Enquist, L.; Hohn, B.; Murray, NE.; Murray, K. Experimental methods for use with lambda. In: Hendrix, RW.; Roberts, JW.; Stahl, FW.; Weisberg, RA., editors. Lambda II. Cold Spring Harbor Laboratory Press; Cold Spring Harbor, NY: 1983. p. 433-366.
- Becker A, Murialdo H. Bacteriophage lambda DNA: the beginning of the end. Journal of Bacteriology. 1990; 172:2819–24. [PubMed: 2140565]
- Bolivar F, Rodriguez R, Greene P, Betlach M, Heyneker H, Boyer H. Construction and characterization of new cloning vehicles. II. A multipurpose cloning system. Gene. 1977; 2:95–113. [PubMed: 344137]
- Cai, ZH. Master's Thesis. University of Iowa; Iowa City, Iowa: 1993. Bacteriophage lambda terminase: analysis of variants with increased packaging efficiency..
- Cai ZH, Hwang Y, Cue D, Catalano C, Feiss M. Mutations in *NuI*, the gene encoding the small subunit of bacteriophage lambda terminase, suppress the postcleavage DNA packaging defect of *cosB* mutations. Journal of bacteriology. 1997; 179:2479–85. [PubMed: 9098042]
- Casjens SR. The DNA-packaging nanomotor of tailed bacteriophages. Nat.Rev.Microbiol. 2011; 9:647–657. [PubMed: 21836625]
- Catalano CE, Cue D, Feiss M. Virus DNA packaging: the strategy used by phage lambda. Mol. Microbiol. 1995; 16:1075–86. [PubMed: 8577244]
- Chattoraj DK, Inman RB. Location of DNA ends in P2, 186, P4 and lambda bacteriophage heads. J.Mol.Biol. 1974; 87:11–22. [PubMed: 4610150]
- Cue D, Feiss M. Genetic analysis of *cosB*, the binding site for terminase, the DNA packaging enzyme of bacteriophage lambda. J. Mol. Biol. 1992; 228:58–71. [PubMed: 1447794]
- Cue D, Feiss M. A site required for termination of packaging of the phage lambda chromosome. Proc. Nat. Acad. Sci., U.S.A. 1993; 90:9290–4.
- Cue D, Feiss M. Genetic analysis of mutations affecting terminase, the bacteriophage lambda DNA packaging enzyme, that suppress mutations in *cosB*, the terminase binding site. J.Mol.Biol. 1992; 228:72–87. [PubMed: 1447796]
- Daniels, D.; Schroeder, J.; Szybalski, W.; Sanger, F.; Coulsen, A.; Hong, D.; Hill, D.; Peterson, G.; Blattner, F. Completed annotated lambda sequence.. In: Hendrix, RW.; Roberts, JW.; Stahl, FW.; Weisberg, RA., editors. Lambda II. Cold Spring Harbor Laboratory Press; Cold Spring Harbor, NY: 1983. p. 519-676.

- de Beer T, Fang J, Ortega M, Yang Q, Maes L, Duffy C, Berton N, Sippy J, Overduin M, Feiss M, Catalano CE. Insights into specific DNA recognition during the assembly of a viral genome packaging machine. *Molecular cell*. 2002; 9:981–91. [PubMed: 12049735]
- Dorgai L, Yagil E, Weisberg RA. Identifying determinants of recombination specificity: construction and characterization of mutant bacteriophage integrases. *J.Mol.Biol.* 1995; 252:178–188. [PubMed: 7674300]
- Feiss M. The bacteriophage DNA packaging machine. *Adv Exp Med Biol*. 2012; 726:489–509. [PubMed: 22297528]
- Feiss, M.; Fisher, R.; Siegele, DA.; Widner, W. Bacteriophage lambda and 21 packaging specificities. In: DuBow, MS., editor. *Bacteriophage Assembly*. Alan R. Liss, Inc.; New York: 1981. p. 213-22.
- Feiss, M.; Catalano, CE. Bacteriophage lambda terminase and the mechanisms of viral DNA packaging.. In: Catalano, CE., editor. *Viral Genome Packaging Machines: Genetics, Structure, and Mechanism*. Landes Bioscience; Georgetown, TX.: 2005. p. 5-39.
- Feiss M, Reynolds E, Schrock M, Sippy J. DNA packaging by lambda-like bacteriophages: mutations broadening the packaging specificity of terminase, the lambda-packaging enzyme. *Genetics*. 2010; 184:43–52. [PubMed: 19841094]
- Fowler RG, Degner GE, Cox EC. Mutational specificity of a conditional *Escherichia coli* mutator, *mutD5*. *Mol. Gen. Genet.* 1974; 133:179–191. [PubMed: 4614067]
- Fujisawa H, Morita M. Phage DNA packaging. *Genes Cells*. 1997; 2:537–545. [PubMed: 9413995]
- Granston AE, Alessi DM, Eades L, Friedman D. A point mutation in the *Nu1* gene of bacteriophage lambda facilitates phage growth in *Escherichia coli* with *himA* and *gyrB* mutations. *Mol. Gen. Genet.* 1988; 212:149–156. [PubMed: 2836702]
- Hwang Y, Feiss M. A mutation correcting the DNA interaction defects of a mutant phage lambda terminase, gpNu1 K35A terminase. *Virology*. 1999; 265:196–205. [PubMed: 10600592]
- Hwang Y, Feiss M. Mutations affecting lysine-35 of gpNu1, the small subunit of bacteriophage lambda terminase, alter the strength and specificity of holoterminase interactions with DNA. *Virology*. 1997; 231:218–230. [PubMed: 9168884]
- Kobayashi I, Murialdo H, Crasemann JM, Stahl MM, Stahl FW. Orientation of cohesive end site *cos* determines the active orientation of *chi* sequence in stimulating *recA*. *recBC*-mediated recombination in phage lambda lytic infections. *Proc.Natl.Acad.Sci.U.S.A.* 1982; 79:5981–5. [PubMed: 6310557]
- Maluf N, Gaussier H, Bogner E, Feiss M, Catalano C. Assembly of bacteriophage lambda terminase into a viral DNA maturation and packaging machine. *Mol. Microbiol.* 2006; 45:15259–15268.
- Maluf N, Yang Q, Catalano C. Self-association properties of the bacteriophage lambda terminase holoenzyme: implications for the DNA packaging motor. *J. Mol. Biol.* 2005; 347:523–542. [PubMed: 15755448]
- Maniatis, t.; Fritsch, EF.; Sambrook, J. *Molecular Cloning, A Laboratory Manual*. Cold Spring Harbor Laboratory Press; Cold Spring Harbor, NY.: 1982.
- Rao, VB.; Feiss, M. *Annual Review of Genetics*. Annual Reviews. Palo Alto; CA: 2008. The bacteriophage DNA packaging motor; p. 647-681.
- Raskin CA, Diaz GA, McAllister WT. T7 RNA polymerase mutants with altered promoter specificities. *Proc.Natl.Acad.Sci.U.S.A.* 1993; 90:3147–3151. [PubMed: 8475053]
- Six E, Klug CAC. Bacteriophage P4: a satellite virus depending on a helper such as prophage P2. *Virology*. 1973; 51:327–344. [PubMed: 4571379]
- Steitz, Thomas A. *Structural Studies of Protein-Nucleic Acid Interaction: The Sources of Sequence-specific Binding*. The Press Syndicate of the University of Cambridge; Cambridge, Great Britain: 1993.
- Sternberg N, Austin S. Isolation and characterization of P1 minireplicons. *Journal of Bacteriology*. 1983; 153:800–812. [PubMed: 6296053]
- Yang Q, Berton N, Manning M, Catalano C. Domain structure of gpNu1, a phage lambda DNA packaging protein. *Biochemistry*. 1999; 38:14238–14447. [PubMed: 10571997]

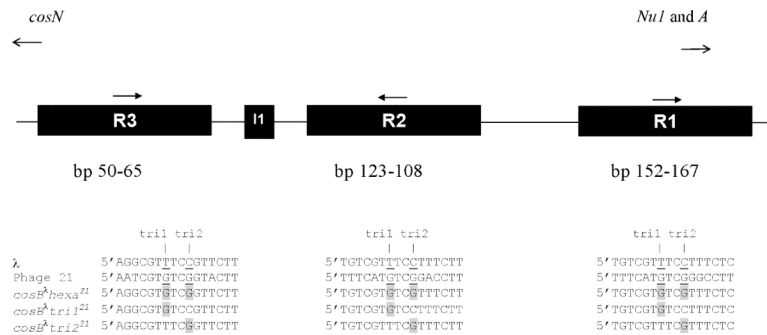


Figure 1. *cosB* Region and Sequences of the R Elements

cosB lies between *cosN* and the terminase genes *NuI* and *A*, and contains three R elements, R3 (bp 50-65), R2 (bp 123-108), and R1 (bp 152-167). The R elements are bound by gpNu1 during packaging initiation. I1, between R3 and R2, is an IHF binding site, the *E. coli* binding/bending protein which folds the DNA so that the major grooves of R3 and R2 face each other, facilitating binding by dimeric gpNu1. The sequence shown for R2 is read 5' to 3' from the bottom strand. R sequences are shown for λ (consensus of 5' tGtCGTTTCCtTTCTt 3'), with the phage-specific bases underlined. The sequences of *cosB^λ hexa²¹*, *cosB^λ tri1²¹*, and *cosB^λ tri2²¹* are also shown, with the changed bp shaded. The *tri1* and *tri2* phage-specific bp, respectively, are in parentheses as follows: R3 (56, 59), R2 (117, 114), and R1 (158, 161).

	support helix	turn	recognition helix	wing
gpNu1	MEVNKKQLADIF	GAS	IRTIQ NWQE	RGGGKGNV...L...
gp1	MKVNKKRLAEIF	NVD	PRTIER WQS	SKGSKGIESV...L...
gpNu1 ^{hy1}	MEVNKKQLADIF	GAS	PRTIER WQS	RGGGKGNV...L...
gpNu1 ^{hy2}	MKVNKKRLAEIF	NVD	PRTIER WQS	RGGGKGNV...L...

Figure 2. gpNu1, gp1, gpNu1^{hy1}, and gpNu1^{hy2} Sequences of the HTH-wing Region

The HTH-wing motif of gpNu1 is involved in *cosB* recognition, and, based on sequence identity, is found in phage 21's gp1. In de Beer *et al.* (de Beer et al., 2002), the support and recognition helices are referred to as α helix A (residues 5-12) and α helix B (residues 16-24), respectively. Residues 31-39 comprise the wing, which also interacts with *cosB* in a non-phage-specific manner (Feiss et al., 2010). The HTH-wing motifs of gpNu1, gp1, gpNu1^{hy1}, and gpNu1^{hy2} are boxed and the bold residues in the recognition helix represent residues that differ between gpNu1 and gp1. For gpNu1^{hy1} and gpNu1^{hy2}, residues derived from gp1 have been shaded for emphasis.

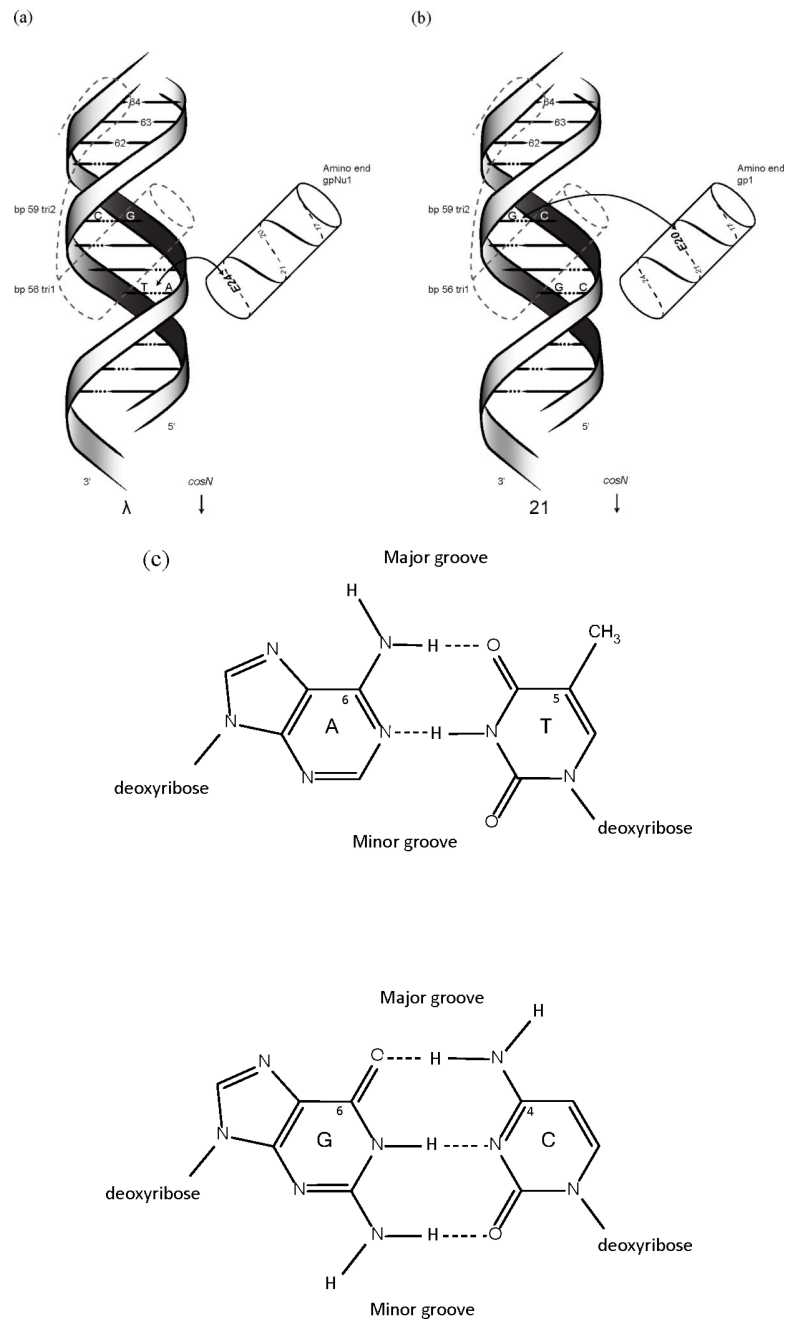


Figure 3. Proposed Orientation of the Recognition Helix of gpNu1 or gp1

Suggested orientation of (a) gpNu1 or (b) gp1 HTH-wing in R3 of their respective *cosB*'s, based on the genetic data of this paper. Dotted lines indicate the placement of the recognition helix and wing on the DNA. The wing extends from the COOH end of the helix and is shown as a loop. On the recognition helix to the right of the DNA, positions of residues E24 (gpNu1) and E20 (gp1) are shown to be on the back side of the helix. Placing the recognition helix in the manner shown situates residues E24^λ and E20²¹ juxtaposed to the phage-specific tri1 (bp 56) and tri2 (bp 59) positions, respectively, and the wing at the narrow groove of bp 62-64, as described in the text. Figure 3 (c) shows positions of

hydrogen bond donors N6 (adenine) and N4 (cytosine), the C5 methyl group of thymine, and O6 of guanine in the major groove of base pairs AT and GC.

Author Manuscript

Author Manuscript

Author Manuscript

Author Manuscript

Table 1

Strains and Plasmids

Genotype	Genotype/Use	Reference
<i>Escherichia coli</i>		
MF1427	C1a <i>galK100 sup⁺</i> , crosses and plaque assay	(Six and Klug, 1973)
MF2979	C1a <i>galK sup⁺</i> (λ^+) plating bacterium for Ap ^R and Kn ^R -transducing assays	(Cue and Feiss, 1992)
MF 2449	C1a <i>zae-13::Tn10 mutD</i>	(Fowler, R.G., G.E. Degner, and E.C. Cox, 1974)
Plasmids		
pJB0	pBR322 carrying λ DNA insert extending from λ bp 44141 to BamHI at 5505. Contains introduced sites for XbaI at 48442 and XmaI at 171.	(de Beer et al., 2002), This paper
pJB0 <i>cosB^λi NuI^λj</i>	<i>i</i> = <i>cosB^{λ+}</i> , <i>cosB^λhexa^{2l}</i> , <i>cosB^λtri1^{2l}</i> , <i>cosB^λtri2^{2l}</i> ; <i>j</i> = <i>NuI⁺</i> , <i>NuI^{hy1}</i> , <i>NuI^{hy2}</i> .	(de Beer et al., 2002), This paper
pJB4 <i>cosB^λi</i>	<i>i</i> = <i>cosB^{λ+}</i> , <i>cosB^λhexa^{2l}</i> , <i>cosB^λtri1^{2l}</i> , <i>cosB^λtri2^{2l}</i>	(de Beer et al., 2002), This paper
Phage *		
λ	λ -P1:5R Kn ^R <i>cI857 nin5</i>	(Chattoraj and Inman, 1974, Sternberg and Austin, 1983).
λ <i>cos2</i>	Phage \times plasmid crosses	(Cue and Feiss, 1992)
λ <i>cosB^λi NuIj</i>	<i>i</i> = <i>cosB^{λ+}</i> , <i>cosB^λhexa^{2l}</i> , <i>cosB^λtri1^{2l}</i> , <i>cosB^λtri2^{2l}</i> ; <i>j</i> = <i>NuI⁺</i> , <i>NuI^{hy1}</i> , <i>NuI^{hy2}</i> .	(de Beer et al., 2002), This paper

* In this phage, the λ site-specific recombination system is replaced by the phage P1 DNA segment encoding the prophage plasmid replication and partitioning functions; the phage also carries a kanamycin resistance cassette which allows one to enumerate phages with yields too low to allow plaque formation, i.e., less than ~10 phages per cell. For simplicity, this phage is designated λ .

Table 2

Burst Sizes* of Phages with Chimeric gpNu1 and *cosBs*

Line	Terminase Allele	<i>cosB</i> Allele				
		<i>cosB^Δ</i>	<i>cosB^{Δ1}</i>	<i>cosB^{Δhexa21}</i>	<i>cosB^{Δtri121}</i>	<i>cosB^{Δtri221}</i>
1	<i>NuI⁺</i>	115 (7.7)	.042 (.007)	11.8 (1.6)	13.8 (2.2)	106 (18.5)
2	<i>NuI^{ph1}</i> (<i>N^ΔH^ΔT^ΔH^Δ</i>)	9.5 (0.7)	100 (14.3)	128 (9.4)	137 (13.3)	145 (7.5)
3	<i>NuI^{ph2}</i> (<i>N^{Δ2}H^{Δ2}T^{Δ2}H^{Δ2}</i>)	.033 (.003)	105 (14.3)	149 (11)	8.4 (1.7)	26.3 (5.7)

* Burst sizes are expressed as phage/induced cell; number in parenthesis is standard error of the mean.

Table 3

Burst Sizes : Pseudorevertants of λ *cosB* ^{λ} *hexa*²¹ *NuI*⁺

<i>cosB</i> ^{λ} or <i>NuI</i> Allele	Burst Size	Number of Independent Isolates	Location (reference)
<i>NuI</i> ⁺ <i>cosB</i> ^{λ}	115 (7.7)	-	-
<i>NuI</i> ⁺ <i>cosB</i> ^{λ} <i>hexa</i> ²¹	11.8 (1.6)	-	-
<i>NuI</i> ⁺ <i>cosB</i> ^{λ} <i>hexa</i> ²¹ L→G ₅₆ T	30.3 (3.4)	17/59	<i>cosB</i> R3 sequence (<i>trf</i> ²¹ site)
<i>NuI</i> ⁺ <i>cosB</i> ^{λ} <i>hexa</i> ²¹ L→C ₁₁₇ A	14.5 (3.1)	3/59	<i>cosB</i> R2 sequence (<i>trf</i> ²¹ site)
<i>NuI</i> ⁺ <i>f</i> ^{E21K}	12.0 (1.8)	1/59	gpNuI recognition helix
<i>NuI</i> ⁺ <i>f</i> ^{E24V}	44.0 (0.4)	1/59	gpNuI recognition helix
<i>NuI</i> ⁺ <i>f</i> ^{E24Q}	53.7 (14.8)	3/59	gpNuI recognition helix
<i>NuI</i> ⁺ <i>f</i> ^{E24K}	59.0 (5.3)	1/59	gpNuI recognition helix
<i>NuI</i> ⁺ <i>f</i> ^{Q25K}	31.2 (8.1)	3/59	Adjacent to gpNuI recognition helix
<i>NuI</i> ⁺ <i>f</i> ^{A14V}	15.4 (0.8)	1/59	Turn of gpNuI HTH (Hwang and Feiss, 1999)
<i>NuI</i> ⁺ <i>f</i> ^{L40F}	63.9 (7.5)	2/59	gpNuI wing (<i>NuI</i> <i>ms1</i> of (Cue and Feiss, 1992), <i>NuI</i> <i>ohm1</i> of (Granston, A.E., D.M. Alessi, L. Eades, and D.Friedman, 1988)
<i>NuI</i> ⁺ <i>f</i> ^{L40I}	127 (8.8)	19/59	gpNuI wing (<i>NuI</i> <i>ms2</i> of (Cue and Feiss, 1992)
<i>NuI</i> ⁺ <i>f</i> ^{Q97K}	61.5 (3.5)	7/59	Holoenzyme assembly? (<i>NuI</i> <i>ms3</i> of (Cue and Feiss, 1992)
<i>NuI</i> ⁺ <i>p</i> ^{104G}	38.0 (6.5)	1/59	Holoenzyme assembly?

Data for *cosB* ^{λ} and *cosB* ^{λ} *hexa*²¹ are taken from Table 2.

* Burst sizes are expressed as phage/induced cell; number in parenthesis is standard error of the mean.

Table 4

Burst Sizes of gpNu1 Replacement Mutants And *Nu1*^{Q20A} Revertant

Replacements in λ -P1 <i>Nu1</i> ⁺	
<i>Nu1</i> Allele	Burst Size
<i>Nu1</i> ⁺	115 (7.7)
<i>Nu1</i> ^{H6P}	81.4 (10.9)
<i>Nu1</i> ^{Q20E}	1.4×10^{-2} (6.3×10^{-3})
<i>Nu1</i> ^{Q20A}	79.8 (6.6)
<i>Nu1</i> ^{N2/R}	132.5 (33.9)
<i>Nu1</i> ^{E2AS}	43.6 (7.0)

Burst sizes are expressed as phage/induced cell; number in parenthesis is standard error of the mean.

Table 5
Yield of Ap^R-Transducing Particles in Cosmid Packaging Assay with pJB4 Cosmids

<i>cosB</i> Allele (Cosmid)	Terminase (Helper phage)					
	<i>NuI</i> ⁺ (normalized)	Proposed Clashes at <i>trfI</i> or <i>trf2</i>	Proposed Favorable Contacts at <i>trfI</i> or <i>trf2</i>	<i>NuI</i> ^{Q20E} (normalized)	Proposed Clashes at <i>trfI</i> or <i>trf2</i>	Proposed Favorable Contacts at <i>trfI</i> or <i>trf2</i>
<i>cosB</i> ^Δ	=100	None	E24 ^Δ - <i>trfI</i> ^Δ	0.33	E20 ²¹ - <i>trf2</i> ^Δ	E24 ^Δ - <i>trfI</i> ^Δ
<i>cosB</i> ^Δ <i>hexA</i> ²¹	1.6	E24 ^Δ - <i>trfI</i> ²¹	None	0.77	E24 ^Δ - <i>trfI</i> ²¹	E20 ²¹ - <i>trf2</i> ²¹
<i>cosB</i> ^Δ <i>trfI</i> ²¹	1.6	E24 ^Δ - <i>trfI</i> ²¹	None	0.022	E20 ²¹ - <i>trf2</i> ^Δ E24 ^Δ - <i>trfI</i> ²¹	None
<i>cosB</i> ^Δ <i>trf2</i> ²¹	42	None	E24 ^Δ - <i>trfI</i> ^Δ	3.3	None	E20 ²¹ - <i>trf2</i> ²¹ E24 ^Δ - <i>trfI</i> ^Δ

Values are Ap^R-transducing particles/cell, from three independent lysates. Packageability is measured by determination of Ap^R-transducing particles produced per cell, as terminase packages using *coses* of plasmid concatemers produced by rolling circle replication.